

Electric Field Distributions of the Fast and Slow Modes Propagated in the Open Rod SiC Waveguide

L. Nickelson, T. Gric, S. Asmontas

Semiconductor Physics Institute, Terahertz's Electronics Laboratory,

A.Gostauto str. 11, LT-01108 Vilnius, Lithuania, phone: +37067103291; e-mail: lucynickelson@gmail.com; nick@pfi.lt

R. Martavicius

Electronics Faculty, Vilnius Gediminas Technical University,

Naugarduko str. 41, LT-03227 Vilnius, Lithuania, phone: +37068556833; e-mail: romanas.martavicius@el.vtu.lt

Introduction

Silicon carbide (SiC) waveguides operating at the microwave range are presently being developed for advantageous use in high-temperature, high-power, and high-radiation conditions. SiC however, has superior properties for power devices, compared to silicon. A change of technology from silicon to silicon carbide will revolutionize the power electronics.

The fabrication of single mode SiC waveguides and the measurement of their propagation loss is reported in [1]. This loss can be used as a benchmark for further development of SiC microphotonic components and circuit for sensor systems [1].

Electrodynamical model of the gyrotropic open circular cylindrical waveguide and its dispersion characteristics are presented in [2].

The circular waveguides can be analyzed using the finite element method. Thus direct and iterative solution techniques of equation systems used in finite element method are analyzed in [3].

A new method for the magnetic field distribution measurement distortions' elimination using gradient-echo double measurement is introduced in [4].

Helical and meander retard systems based on the multiconductor lines with the complex cross-sections using multiconductor line method are considered in [5].

We present here results of electrodynamic analysis of the open circular rod ceramic (composite) SiC waveguide (see Fig.1). The solution of the Maxwell's equations has been carried out by method of partial areas [6]. We have already made the electrodynamic analysis of some circular cylindrical gyrotropy waveguides [7, 8].

Here we for the first time investigate the complex propagation constants \underline{h} of the main and higher modes propagated in the open waveguide made of very lossy material. We also study the propagation of fast mode for the first time. Here we analyze two slow modes and a one fast mode. In order to examine the behavior of complex

value \underline{h} we look for complex roots of the complex dispersion equation. For this reason we used the modified Muller method. We carried out a stability test of our algorithm and made the algorithm regularization when the material losses were quite large. The solution of this electrodynamic problem and the approbation of our computer algorithm are given in our articles [6–8]. The numerical results of the SiC waveguide investigations are presented at the temperature $T = 1800^{\circ}\text{C}$. The permittivity of SiC material is $\underline{\epsilon}_r^{\text{SiC}} = 11 - 7i$ [9]. We have accepted that this value of permittivity $\underline{\epsilon}_r^{\text{SiC}}$ corresponds to the frequency 12.5 GHz. In the present article the azimuthal index characterizing azimuthal variations of the electric field is $m = 1$. We have created a computer algorithm with 2D graphical visualization in the MATLAB language.

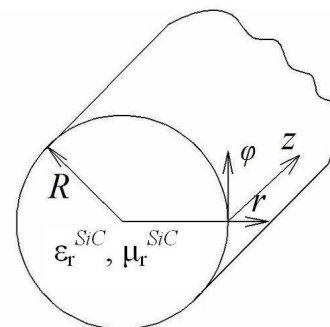


Fig. 1. The SiC waveguide model

Dispersion characteristics and electric field distributions

The dependences of the real part $h' = \text{Re}(\underline{h})$ and imaginary part (propagation losses) $h'' = \text{Im}(\underline{h})$ of the

complex propagation constant $\underline{h} = h' - ih''$ of the SiC waveguide with the radius $R = 2.5$ mm when $T = 1800^\circ\text{C}$ on the operating frequency f are presented in Fig. 2 (a) and (b).

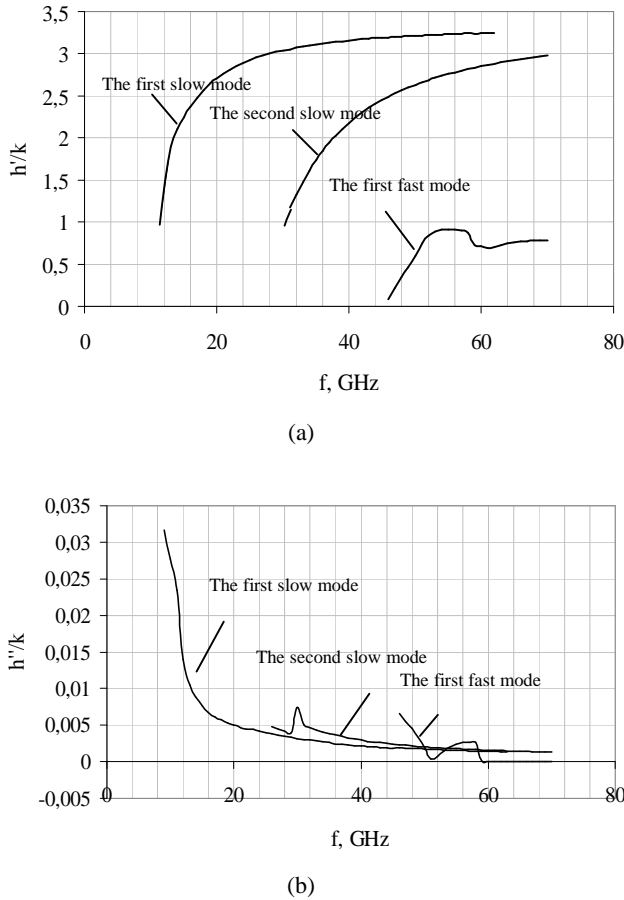


Fig. 2. Dispersion characteristics of the SiC waveguide

There are dispersion curves of three waveguide modes in Fig. 2. The main and first higher waveguide modes are slow modes, because their $h'/k > 1$. The third depicted mode is a first slow mode because the value $h'/k < 1$ for this mode.

The cutoff frequencies of the two slow modes are $f_{cut} = 12.5$ GHz and 30 GHz respectively. The cutoff frequency of the first fast mode is $f_{cut} = 46$ GHz.

The propagation losses of all analyzed modes (see Fig. 2 (b)) were calculated in the assumption that the imaginary part of the complex permittivity $\text{Im}(\epsilon_r^{\text{SiC}})$ is equal to 7 at the operating frequency 12.5 GHz. The value $\text{Im}(\epsilon_r^{\text{SiC}})$ decreases when the operating frequency f increases, because this magnitude is inversely proportional to the value f . Analyzing the propagation losses of the slow and fast modes we see that the first slow mode has the largest propagation losses in the region of its cutoff frequency. We see peaks on the losses' curves of the second and third modes. Our researches have shown that a position of these peaks depends on the waveguide radius also. At smooth reduction of waveguide radius the peak of propagation losses will be smoothly displaced to the right side on a scale of frequencies.

The electric field distributions of the slow and fast modes are presented in Figs 3-5. The distributions of the electric field were calculated in 10000 points. The electric field strength lines are presented in Figs 3(a) – 5(a). Visualizations of the electric field intensity are shown in Figs 3(b) – 5(b).

The values of the electric E_r, E_φ, E_z and magnetic H_r, H_φ, H_z field components of these modes are presented in Table 1.

Table 1. The electromagnetic field components in the fixed point ($r = 2.4$ mm, $\varphi = 0$, $z = 0$) of the SiC waveguide cross-section when $T = 1800^\circ\text{C}$

<i>Slow modes</i>						
<i>The main</i>	$m = 1, f = 15$ GHz					
	$E_r, \text{V/m}$	$E_\varphi, \text{V/m}$	$E_z, \text{V/m}$	$H_r, \text{A/m}$	$H_\varphi, \text{A/m}$	$H_z, \text{A/m}$
	$2.2 \cdot 10^{-2} - 8 \cdot 10^{-3}i$	$3.9 \cdot 10^{-2} + 4 \cdot 10^{-2}i$	$8 \cdot 10^{-2} + 1.46 \cdot 10^{-1}i$	$-5.943 \cdot 10^{-4} - 6.49 \cdot 10^{-4}i$	$-1.6 \cdot 10^{-5} + 4.267 \cdot 10^{-5}i$	$4.148 \cdot 10^{-4} - 4.424 \cdot 10^{-4}i$
<i>The first higher</i>	$m = 1, f = 50$ GHz					
	$E_r, \text{V/m}$	$E_\varphi, \text{V/m}$	$E_z, \text{V/m}$	$H_r, \text{A/m}$	$H_\varphi, \text{A/m}$	$H_z, \text{A/m}$
	$1.349 \cdot 10^{-4} - 1.582 \cdot 10^{-4}i$	$1.554 \cdot 10^{-4} + 1.204 \cdot 10^{-4}i$	$4.205 \cdot 10^{-4} + 3.623 \cdot 10^{-4}i$	$-1.604 \cdot 10^{-6} - 1.127 \cdot 10^{-6}i$	$1.32 \cdot 10^{-6} - 1.643 \cdot 10^{-6}i$	$8.011 \cdot 10^{-7} - 1.115 \cdot 10^{-6}i$
<i>Fast mode</i>						
<i>The second higher</i>	$m = 1, f = 51$ GHz					
	$E_r, \text{V/m}$	$E_\varphi, \text{V/m}$	$E_z, \text{V/m}$	$H_r, \text{A/m}$	$H_\varphi, \text{A/m}$	$H_z, \text{A/m}$
	$2.5 \cdot 10^{-2} - 1.4 \cdot 10^{-2}i$	$2 \cdot 10^{-2} - 1.6 \cdot 10^{-2}i$	$2.95 \cdot 10^{-1} - 3 \cdot 10^{-2}i$	$-3.434 \cdot 10^{-4} + 6.650 \cdot 10^{-5}i$	$10^{-3} - 10^{-3}i$	$-2.887 \cdot 10^{-4} + 1.958 \cdot 10^{-4}i$

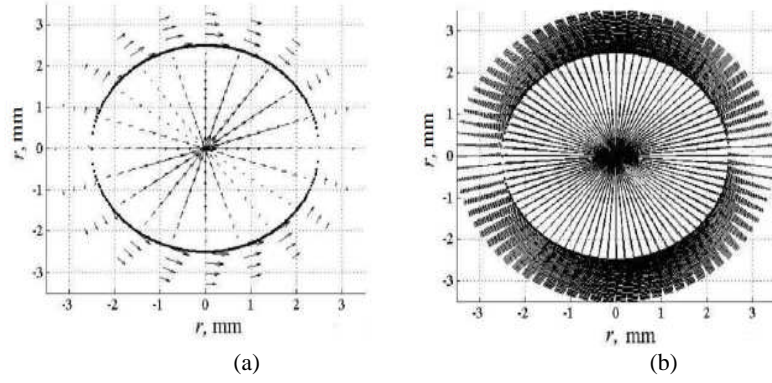


Fig. 3. The electric field distribution of the first slow mode propagating in the SiC waveguide at $f = 15$ GHz

The electric field distributions of the first slow mode (the main mode) are presented in Fig. 3.

We should notice that the electric field distribution of the first slow mode depicted in Fig. 3 (a) is rotated clockwise by 90 degrees respectively to the electric field distribution of the same mode propagated in the analogical waveguide made of lossless material SiC with $\text{Im}(\epsilon_r^{\text{SiC}})=0$. In Fig. 3 (a) we can see that electric field

strength lines are directed clockwise in the I and II quarters and counterclockwise in the III and IV quarters. The electric field strength lines are directed radially inside the SiC waveguide. We see that there is only one variation of the electric field on the waveguide radius. In Fig. 3 (b) we can see that the strongest electric field concentrates in the two areas. These ones are in the waveguide center and on the waveguide boundary.

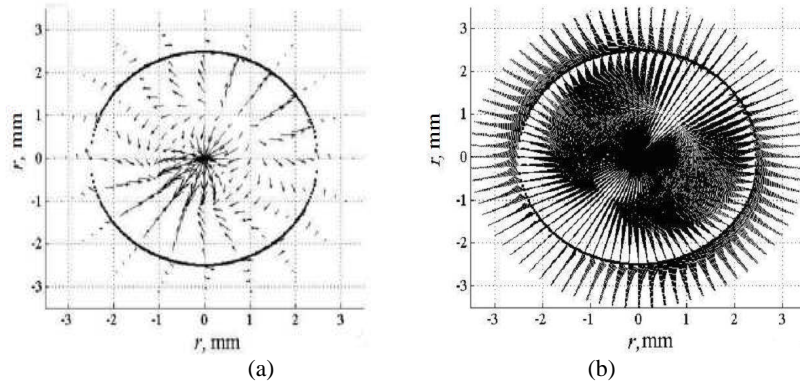


Fig. 4. The electric field distribution of the second slow mode propagating in the SiC waveguide at $f = 50$ GHz

In Fig. 4 we can observe an interesting behavior of the electric field distribution of the second slow mode (the first higher waveguide mode) inside the SiC waveguide as well as outside it close to its boundary. In Fig. 4 (a) we see that there are two variations of the electric field on the waveguide radius. The electric field intensity distribution inside the waveguide has an intricate picture of a shape of

two lobes. We see that when the distance from the waveguide becomes larger the electric field becomes smaller outside the waveguide. We should notice that there is a third slow mode (the third waveguide mode) in the frequency range of 1 – 100 GHz. The cutoff frequency of this mode is $f_{cut} = 51$ GHz. The analysis of the third slow mode is beyond this article.

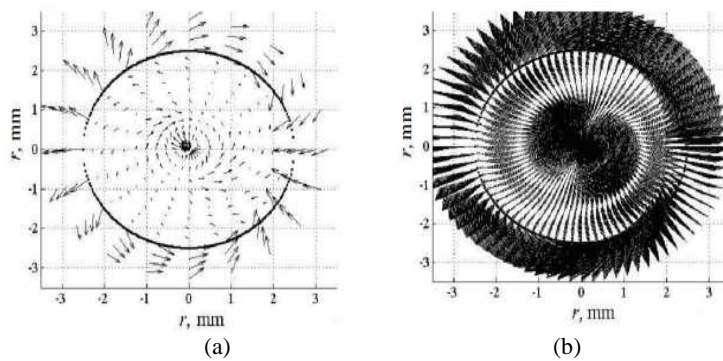


Fig. 5. The electric field distribution of the first fast mode propagating in the SiC waveguide $f = 51$ GHz

In Fig. 5 (a) we can see that the electric field strength lines of the first fast mode (the second higher waveguide mode) have three variations by the radius. In Fig. 5 (b) we can observe that the electric field distribution of the first fast mode inside the SiC waveguide is in the form of two lobes. The strongest electric field concentrates outside the waveguide. The number of variations of a field along the waveguide radius for all the modes corresponds to the nowadays understanding about the main and higher mode of dielectric waveguides. The comparison of Fig. 3-5 shows us that the electric field distributions are strongly different.

Conclusions:

1. We investigated the two slow and one fast modes that can propagate in the SiC rod waveguide with the radius $R = 2.5$ mm at the temperature 1800°C in the frequency range of 1 – 100 GHz. The distribution of electric field is very different for every investigated mode.
2. The electric field of the second slow mode is the strongest in the center of the waveguide. Therefore the breakdown energy can be lower for this waveguide mode.
3. The strongest electric field of the first slow mode concentrates in the air, close to the SiC waveguide border.
4. The propagation losses of the first slow mode are the largest in comparison to the losses of other two modes closed to the cutoff frequency.

References

1. **Pandraud G., Pham H. T. M., French P. J., Sarro P. M.** PECVD SiC optical waveguide loss and mode

Received 2009 02 10

L. Nickelson, T. Gric, S. Asmontas, R. Martavičius. Electric Field Distributions of the Fast and Slow Modes Propagated in the Open Rod SiC Waveguide // Electronics and Electrical Engineering. – Kaunas: Technologija, 2009. – No. 5(93). – P. 87–90.

Here we present the electrodynamic analysis of the ceramic circular rod silicon carbide (SiC) waveguide with the radius $R = 2.5$ mm at the temperature 1800°C . We present dispersion characteristics of the SiC waveguide in the frequency range 1–100GHz. We show the losses of two slow and one fast waveguide modes. We give here the electric field distributions of the slow and fast modes propagated in the investigated waveguide. We present a table with magnitudes of the electric and magnetic field components in the fixed point of the SiC waveguide cross-section. Ill. 5, bibl. 9 (in English; summaries in English, Russian and Lithuanian).

Л. Никельсон, Т. Гриц, С. Ашмонтас, Р. Мартавичюс. Распределения электрических полей быстрых и медленных мод, распространяющихся в открытом стержневом SiC волноводе // Электроника и электротехника. – Каунас: Технология, 2009. – № 5(93). – С. 87–90.

Представлен электродинамический анализ керамического круглого стержневого силикон карбидного (SiC) волновода с радиусом $R = 2.5$ мм при температуре 1800°C . Мы представили потери двух медленных и одной быстрой моды. В статье помещены дисперсионные характеристики SiC волновода в частотном интервале 1–100GHz. В работе показаны распределения электрических полей медленной и быстрых мод, распространяющихся в исследуемом волноводе, а также дана таблица значений компонент электрического и магнитного полей в фиксированной точке сечения SiC волновода. Ил. 5, библи. 9 (на английском языке, рефераты на английском, русском и литовском яз.).

L. Nickelson, T. Gric, S. Ašmontas, R. Martavičius. Lėtųjų ir greitųjų modų, sklindančių atviraime strypiniame SiC bangolaidyje, elektrinių laukų pasiskirstymai // Elektronika ir elektrotechnika. – Kaunas: Technologija, 2009. – Nr. 5(93). – P. 87–90.

Pateikta keraminio apskritiminio strypinio silikoninio karbidinio (SiC) bangolaidžio, kurio spindulys $R = 2,5$ mm, elektrodinaminė analizė, atlikta esant 1800°C temperatūrai. Pateikiami dviejų lėtųjų ir vienos greitosios modų nuostoliai, bei SiC bangolaidžio dispersinės charakteristikos 1–100 GHz dažnių ruože ir lėtųjų bei greitųjų modų, sklindančių nagrinėjamame bangolaidyje, elektrinių laukų pasiskirstymai. Taip pat pateikta elektrinių ir magnetinių laukų reikšmių, gautų SiC bangolaidžio skerspjūvio fiksuotame taške, lentelė. Il. 5, bibl. 9 (anglų kalba; santraukos anglų, rusų ir lietuvių k.).

characteristics // Optics and Laser Technology, 2007. - No. 3(39). – P. 532–536.

2. **Asmontas S., Nickelson L., Malisauskas V.** Investigation of magnetized semiconductor and ferrite waveguides // Electronics and Electrical Engineering, 2006. - No. 2(66). – P. 56-61.
3. **Tarvydas P., Noreika A.** Usability Evaluation of Finite Element Method Equation Solvers // Electronics and Electrical Engineering, 2007. - No. 2(74). – P. 13-16.
4. **Andris P., Frollo I.** Elimination of Distortions in Static Magnetic Field Distribution Measurements // Electronics and Electrical Engineering, 2008. - No. 2(82). – P. 9-12.
5. **Burokas T., Staras S.** Properties of the Retard System Models Based on the Complex Cross Section Multiconductor Lines // Electronics and Electrical Engineering, 2008. - No. 4(84). – P. 3-8.
6. **Nickelson L., Gric T., Asmontas S., Martavičius R.** Electrodynamic analyses of dielectric and metamaterial hollow-core cylindrical waveguides // Electronics and Electrical Engineering, 2008. - No. 2(82). – P. 3-8.
7. **Nickelson L., Gric T.** Dispersion characteristics and electric field distributions of modes propagating in the open electrically gyrotropic semiconductor rod waveguide // Proceedings of 17th Intern. Conf. on Microwaves, Radar and Wireless Communications, MIKON-2008, 19–21 May 2008, Wrocław, Poland, 2008. - Vol. 2. – P. 577-580.
8. **Nickelson L., Asmontas S., Malisauskas V., Shugurov V.** The open cylindrical gyrotropic waveguides. – Vilnius: Technika, 2007. - 248 p. (in Lithuanian).
9. **Baeraky T. A.** Microwave Measurements of the Dielectric Properties of Silicon Carbide at High Temperature // Egypt. J. Sol., 2002. - No. 2(25). – P.263-273.